Spectroscopic characterization of GEO satellites with Gunma LOW resolution Spectrograph

Takao Endo, Hitomi Ono, Mana Hosokawa and Toshiyuki Ando

Mitsubishi Electric Corporation, Information Technology R&D Center

Takashi Takanezawa

Mitsubishi Electric Corporation, Communication Systems Center

Osamu Hashimoto

Gunma Astronomical Observatory

ABSTRACT

The spectroscopic observation is potentially a powerful tool for understanding the Geostationary Earth Orbit (GEO) objects. We present here the results of an investigation of energy spectra of GEO satellites obtained from a ground-based optical telescope. The spectroscopic observations were made from April to June 2016 with the Gunma LOW resolution Spectrograph and imager (GLOWS) at the Gunma Astronomical Observatory (GAO) in JAPAN. The observation targets consist of eleven different satellites: two weather satellites, four communications satellites, and five broadcasting satellites. All the spectra of those GEO satellites are inferred to be solar-like. A number of well-known absorption features such as H-alpha, H-beta, Na-D, water vapor and oxygen molecules are clearly seen in the wavelength range of 4,000 - 8,000 Å. For comparison, we calculated the intensity ratio of the spectra of GEO satellites to that of the Moon which is the natural satellite of the earth. As a result, the following characteristics were obtained. 1) Some variations are seen in the strength of absorption features of water vapor and oxygen originated by the telluric atmosphere, but any other characteristic absorption features were not found. 2) For all observed satellites, the intensity ratio of the spectrum of GEO satellites decrease as a function of wavelength or to be flat. It means that the spectral reflectance of satellite materials is bluer than that of the Moon. 3) A characteristic dip at around 4,800 Å is found in all observed spectra of a weather satellite. Based on these observations, it is indicated that the characteristics of the spectrum are mainly derived from the solar panels because the apparent area of the solar cell is probably larger than that of the satellite body.

1. INTRODUCTION

Space Situational Awareness (SSA) is a concept about security in the outer space, in order to ensure the safety of the space flight, understand the current status of the satellites, prevent collision, or understand the status of the space debris, etc. The motions of the space debris are mainly observed by radio wave (radar) and optic (telescope), and then cataloged as the orbital elements.

On the other hand, the Geostationary Earth Orbit (GEO) objects cannot be spatially resolved even by current large aperture ground-based optical telescopes since they are located at a long distance from the ground. Therefore, unresolved optical measurements such as spectroscopy can be a good tool for understanding individual characteristics of each GEO object. In practice, optical properties other than motion, such as luminance, time variation of luminance, or spectral reflectance, are regarded as media to guess the size, materials, and rotation of the target. In this paper, we report the results of investigations of energy spectra of eleven GEO satellites: weather satellites, communications satellites, and broadcasting satellites obtained with the use of the 1.5 m telescope at Gunma Astronomical Observatory (GAO).

2. OBSERVATION PLAN

2.1. INSTRUMENTATION

The 1.5 m telescope at GAO which is located about 120 km northwest of Tokyo was used for a spectral analysis of GEO objects because a telescope with a large aperture enables to collect a large amount of light. The specifications and performances of the 1.5 m telescope at GAO are listed in Table 1 [1; 2]. This telescope has no tracking capability for high-speed moving objects such as the Low Earth Orbit (LEO) objects, because the alt-azimuth mount was designed only for sidereal tracking.

In case of the GEO object observation, the pointing direction of the reflector (AZ: azimuth angle, EV: elevation angle) is fixed, and then GEO object remains stationary in the camera field of view. The GEO object is therefore observed without any type of tracking. In practice, a manual adjustment for object tracking is required because the position of GEO object slightly drifts during the exposure for about 10 minutes or less.

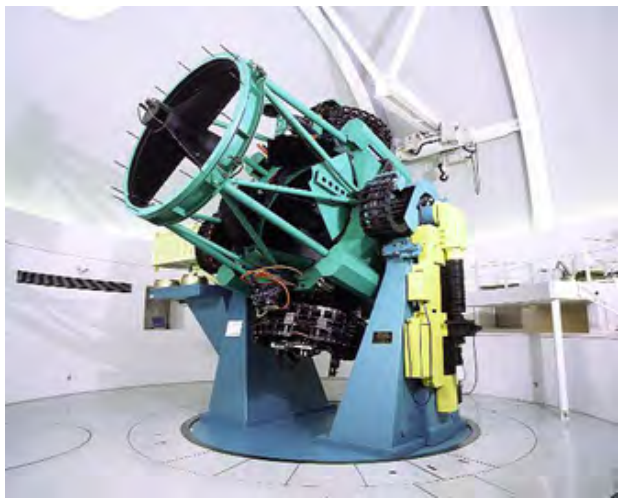

Fig. 1. 1.5 m reflector at Gunma astronomical observatory.

For various scientific research, three kinds of instruments are placed at the three different focal planes of the 1.5 m reflector. In the following observations, we used the Gunma LOW resolution Spectrograph and Imager for optical wavelength (GLOWS). Specifications and performances of GLOWS are listed in Table 2.

GLOWS is the spectroscopic instrument combined grism and CCD camera. It provides a $\lambda/\Delta\lambda = 300 \sim 500$ resolving power in the visible wavelength range of $\lambda = 4,000 \sim 8,000$ Å. Grism is the optical element which is composed of diffraction grating and prism, and is useful in spectrometers that requires in-line presentation of the spectrum. The light diffracted by the grating is bent back in line by the refracting effect of the prism.

In order to avoid the contamination source close to the observation target, the target should be located in the center of narrow slit at the spectrographs entrance. Then the grism creates a dispersed spectrum centered on the location of the object in the camera field of view. The dispersion direction is perpendicular to the slit and the spatial direction along the slit. In the GLOWS instrument, arc line lamps (FeNeAr) are contained for the pixel-to-wavelength conversion.

2.2. SOLAR RADIATION SPETRUM

The red line in Figure 2 shows an example of solar radiation spectrum obtained at Tsukuba 12:10 (JST) on 11 May 2012 at the elevation corresponding to the airmass = 1.1 [3]. The horizontal axis shows the wavelength, the vertical

Table 1. 1.5 m reflector at Gunma astronomical observatory.

Item	Specification
Optics	Ritchey-Chretien
Diameter of primary mirror	160 cm
Effective diameter	150 cm
Focal length	1830 cm (F/12.2)
Hartmann constant	0.3″
Mounting	Altazimuth
Pointting accuracy	3″ (rms)
Tracking accuracy	0.7″ (rms) (15 min)
Diameter of Dome	11 m
Establish	March 1999
Manufacturer	Mitsubishi Electric Corp.

axis shows spectral irradiance. Absorption features such as Hα, Hβ, Na-D (λ = 5,896 Å) and iron are clearly seen in solar spectrum. It is well known that such spectral features are originated from the solar atmosphere. On the other hand, absorption features such as O_2 and H_2O are also clearly seen, which are caused by the absorption of atmosphere surrounding the Earth.

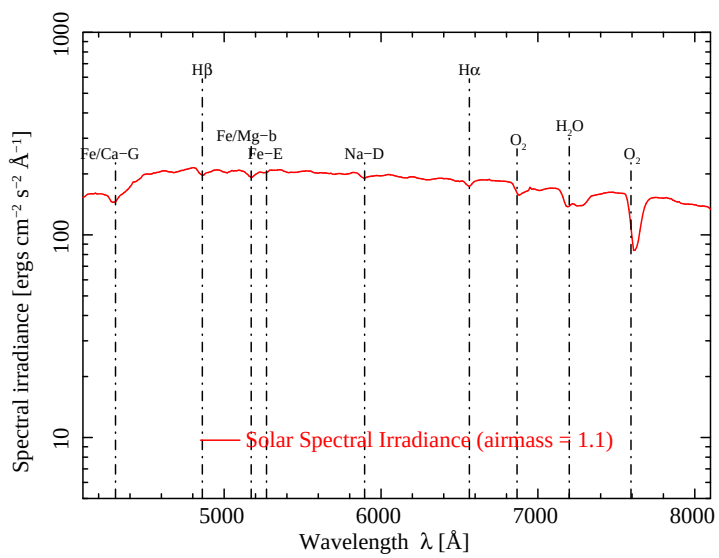

Fig. 2. Example of solar spectrum (2012/5/11 12:10).

2.3. THE SURFACE REFLECTANCE OF COMMON SATELLITE MATERIALS

As the artificial satellites shine brightly by mainly reflection of sunlight, it is important to know the spectral reflectance of typical materials of artificial satellites. At first, we obtained samples of Multi-Layer Insulation (MLI), mono-crystalline silicon cells (solar panel), and Carbon Fiber Reinforced Plastic (CFRP), and then measured the spectral

Table 2. Gunma LOW resolution Spectrograph and imager (GLOWS).

Item	Specification
Detector	Andor DW432
	(e2v CCD55-30 Back-illumination: 1250×1152)
	$0.6''$ / pixel $\rightarrow$ FOV: $10'$
Coverage	$4,000 \sim 8,000$ Å
Imaging	4 filter positions (+ hole) : B, V, R, I
Disperser	Grism
Resolution	$400 \sim 500$
Slit	$40''$ (length), $1.8''$ (width)
Cooler	3 stage pertier
Comparison	Fe, Ar, Ne
Manufactuerer	GENESIA Corp.

reflectances [4]. The measured samples are listed in Table 3.

Table 3. Sample list [4].

Sample	Surface characteristics
Multi layer Insulation (MLI)	Gold & silver, smooth surface
Mono-crystalline Silicon Cells (solar panel)	Black, smooth surface
Carbon Fiber Reinforced Plastic (CFRP)	Black, rough surface

In Figure 3, we plot the logarithm of the spectral reflectivity against wave length for the samples in Table 3. The incident angle to the normal of sample plane is set to 15°. The broken lines, dot-dashed lines and solid lines show the s-polarized, p-polarized and averaged light, respectively. The passbands of the Johnson's *UBVRI* photometry are plotted as dotted lines. And yellow lines, blue lines and black lines show the reflectance of MLI, solar panel and CFRP, respectively.

From the Figure 3, we can see that the reflectance of MLI is in proportion to the wave length from B band to V band. The solar panel, on the other hand, is inverse proportion to the wave length in the B-V bands. The data of solar panel are intentionally hidden in R band because characteristic features are seen in this sample. This is probably due to the surface material of the multilayer coatings.

3. OBSERVATIONS

3.1. THE OBSERVATION JOURNAL

First of all, the observation journal of GEO satellite targets obtained with GLOWS are listed in Table 4. Note that we chose these targets based on their location, as they were located within the longitude range ±60° from +135° of east longitude, and whose orbital inclination were smaller than 1°. These spectroscopic observations were carried out from April through June 2016. For each target, ten single frames with an exposure time of 120 seconds were obtained.

In order to compare the observed spectra with others, we also observed the standard stars and the Moon spectra. The

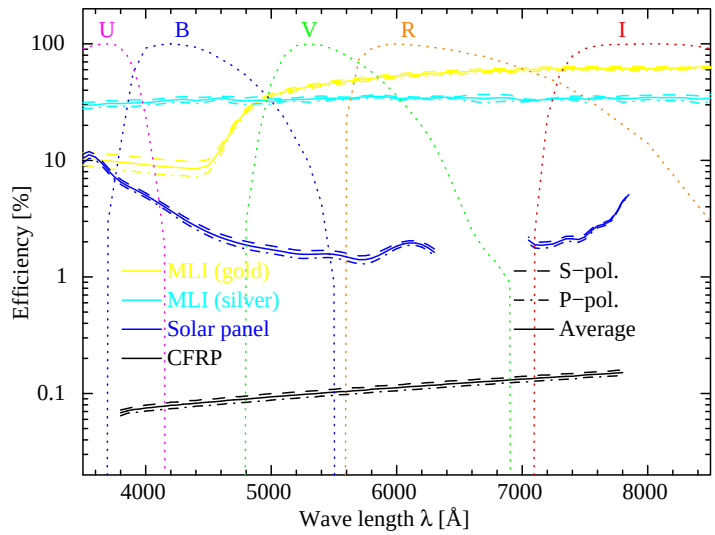

Fig. 3. Spectral reflectance of typical materials.

observation journal both of the standard stars used for calibrations and the Moon whose spectra is similar to the Sun, are also listed in Table 4.

3.2. ELECTRICAL POWER AND SOLAR PANEL SPAN

Table 5 shows the electrical power and the solar panel span of observed GEO satellites [5]. Note that the electrical power used by optical satellites is generally smaller than that of communications and broadcasting satellites. In Table 5, the electrical power used by weather satellites is smaller than that of communications and broadcasting satellites. In practice, the weather satellites MTSAT2 (HIMAWARI-7) and HIMAWARI-8 have only 3 (not larger than 10 m) and 2 (2.8 m $\times$ 2) solar panels on one side of their satellite bus, respectively.

4. SPECTRAL ANALYSIS

4.1. SPECROSCOPIC DATA REDUCTION

We have carried out standard data reductions using the bias, dark and flat field frames. In order to obtain the flux calibrated spectrum, we have observed the spectroscopic standard stars HR4468 and HR5501 as well at almost the same elevation angles where the observations of the target satellites were made. The spectrum of these standard stars are well-known based on standard star database. By comparing with the spectra of standard stars, the flux calibrated spectra of target satellites are calculated.

In order to evaluate the systematic error of these correction, we calculate the spectrum normalized by the averaged intensity in the spectral range of $5,000 \sim 7,000$ Å. The normalized spectra of standard stars are plotted against the wavelength in Figure 4. Except for the spectral range of $< 4,500$ Å and around well-known absorption lines, the systematic deviations of the data from the average are less than 10 % as shown in Figure 5. Hereafter, we estimate the systematic error of these spectral correction is kept less than 10 %.

Table 4. The observation journal.

I.D.	Observation time (JST)	Object		Category	Exposure [s]	Elevation [°]
1 . .	2016/4/26 20:15 – 20:45	MTSAT-2	2006-004A	weather	1,200	47.2
2 . .	2016/4/26 20:52 – 21:28	HIMAWARI-8	2014-060A	weather	1,200	47.6
3 . .	2016/4/26 21:47 – 22:46	SUPEBIRD-B2	2000-012A	communication	1,200	41.1
4 . .	2016/4/26 21:32 – 21:34	HR4468	–	standard star	50	42.9
5 . .	2016/4/26 21:37 – 21:39	HR4468	–	standard star	50	42.8
6 . .	2016/5/18 21:21 – 21:50	HIMAWARI-8	2014-060A	weather	1,200	47.6
7 . .	2016/5/18 21:59 – 22:28	SUPEBIRD-C2	2008-038A	communication	1,200	47.3
8 . .	2016/5/18 22:35 – 22:39	HR5501	–	standard star	100	54.1
9 . .	2016/5/18 22:40 – 22:45	HR5501	–	standard star	100	54.1
10 .	2016/5/18 22:52 – 23:20	N-SAT-110	2000-060A	broadcast	1,200	33.8
11 .	2016/5/18 23:33 – 24:04	JCSAT-2A	2002-015A	communication	1,200	44.7
12 .	2016/5/18 24:08 – 24:38	JCSAT-5A	2006-010A	communication	1,200	46.9
13 .	2016/5/18 24:43 – 25:12	JCSAT-3A	2006-033A	broadcast	1,200	46.0
14 .	2016/5/18 25:24 – 25:51	JCSAT-RA	2009-044A	broadcast	1,200	46.0
15 .	2016/5/18 26:01 – 26:29	JCSAT-4B	2012-023A	broadcast	1,200	44.7
16 .	2016/5/23 21:20 – 21:23	HR5501	-	standard star	50	51.1
17 .	2016/5/23 21:46 – 22:16	HIMAWARI-8	2014-060A	weather	1,200	47.6
18 .	2016/5/23 22:49 – 22:51	Moon	–	reference	3	26.0
19 .	2016/6/2 22:05 – 22:10	HR5501	–	standard star	100	53.8
20 .	2016/6/2 22:16 – 22:46	BSAT-3C	2011-041B	broadcast	1,200	37.7
21 .	2016/6/2 22:51 – 23:20	HIMAWARI-8	2014-060A	weather	1,200	47.5
22 .	2016/6/5 22:35 – 22:41	HR5501	–	standard star	100	51.3
23 .	2016/6/5 22:46 – 23:15	HIMAWARI-8	2014-060A	weather	1,200	47.5

4.2. ENERGY SPECTRA OF THE GEO SATELLITES

After the correction described in section 4.1, we compare the flux calibrated spectra of GEO satellites. Figures 6 – 8 compare the energy spectra of GEO satellites observed with GLOWS in the visible spectral range. The source fluxes of communications satellites are plotted against the wavelength in Figure 6. In the same way, the Figure 7 and Figure 8 show the spectra of broadcasting and weather satellites, respectively. Especially, the weather satellite HIMAWARI-8 was observed with GLOWS five times in the period from April through June.

For all spectra of GEO satellites obtained from GLOWS, the well-known absorption lines such as Hα, Hβ, Na-D, water vapor and oxygen are clearly seen. Compared with the solar radiation spectrum as shown in Figure 2, the spectral distribution of GEO satellites is also very similar to that of the solar spectrum.

Next, we compare with the spectra of the same satellite target obtained at another day observations as shown in Figure 8. Although the strength of atmospheric absorption varies day by day, there is no significant spectral difference in the visible wavelength range. Any systematic deviations of atmospheric correction can be negligible.

Table 5. Electrical power and solar panel span.

Satellite name	Bus	Size [m]	Electrical power [kW]	Solar panel span [m]
JCSAT-2A	Boeing 601	$2.7 \times 3.6 \times 4.3$	3.7	-
JCSAT-5A	A2100AX	-	4	26.9
Superbird-B2	Boeing 601 HP	$2.7 \times 3.6 \times 4.0$	5.5	26
Superbird-C2	DS2000	$6.3 \times 3.7 \times 3.0$	8.0	31.6
N-SAT-110	A2100AX	-	8.3	26
JCSAT-3A	A2100AX	-	4	26.9
JCSAT-RA	A2100AX	-	4	26.9
JCSAT-4B	A2100AX	-	-	-
BSAT-3C	A2100A	-	7.5	-
MTSAT-2	DS2000	$2.4 \times 2.6 \times 2.6$	3.4	($\sim$ 10)
HIMAWARI-8	DS2000	$2.2 \times 2.1 \times 2.0$	2.6	(2.8×2)

A spectrum of the Moon observed by GLOWS is presented in Figure 9, which is almost the same as the solar spectrum since the Moon shines reflecting the sunshine.

5. DISCUSSION

As described in section 4.2, the obtained spectrum of both GEO satellites and the Moon are similar to the solar spectrum. We introduce a spectrum ratio between the GEO satellites and the Moon. Figures 10 – 13 show the spectrum ratios of communications satellites, broadcasting satellites, and weather satellites, respectively. In these spectrum ratios, absorption features such as Hα, Hβ and Na-D lines cannot be seen. Since both the satellites and Moon are shining by reflecting solar light which contains those spectral features originated in the solar surface, they are canceled by dividing the satellite spectrum by the spectrum of the Moon. This result indicates that the spectrum ratio is useful enough to investigate the material properties of the GEO satellites.

On the other hand, since the strength of atmospheric absorption is different in each observation, residuals of the absorption features such as water vapor and oxygen originated by the Earth's atmosphere are remained even in the spectrum ratios. No other characteristic absorption features are found.

In addition, by excluding the data affected by the large atmospheric absorption at wavelengths shorter than 4, 500 Å, the slope of spectrum ratios shown in Figures 10 – 13 are generally decreasing, or flat against the wavelength. It means that the spectral reflectance of satellite materials is bluer than that of the Moon. In the spectrum ratios of HIMAWARI-8 as shown in Figure 12, we can clearly see the characteristic dip around 4,800 Å. However, we couldn't detect such a characteristic dip found in HIMAWARI-8 in the spectrum ratios of communications satellites, broadcasting satellites and MTSAT-2 as shown in Figures 10, 11 and 13, respectively.

In order to convert sunlight into electricity, solar panels of GEO satellite are extended and oriented towards the Sun. Depending on the phase angle defined as the angle between the ray from the Sun to the satellite and the line of sight to satellite, the projected area of solar panels are generally expected to be larger than that of the satellite body. Therefore, it is assumed that the amount of reflected light from solar panels is significantly larger than that from the satellite bus. Since the reflectivity of solar panels decreases against the wavelength as shown in Figure 3, we thus consider that the

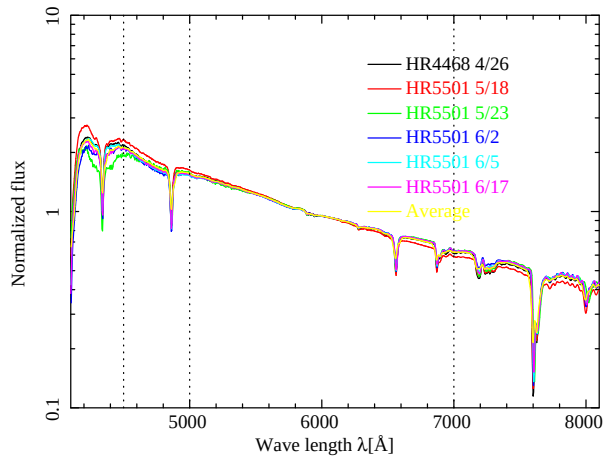

Fig. 4. Energy spectra of standard stars.

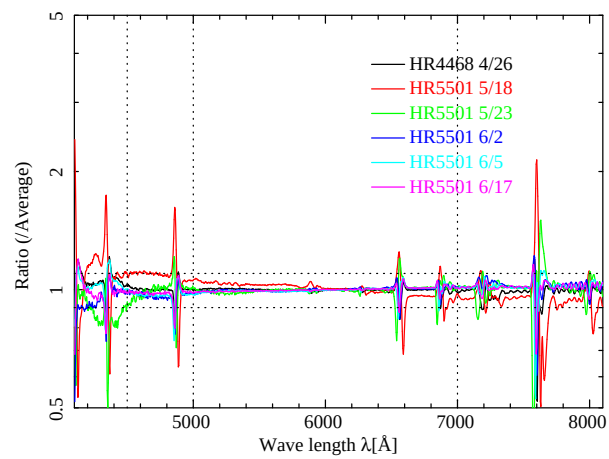

Fig. 5. The deviations of the standard star spectra.

observed spectrum ratios of GEO satellites in Figures 10 – 13, except for the characteristic dip as discussed later, are also generally decreasing or flat against wavelength.

The characteristic dip around 4,800 Å can be clearly seen in every spectrum ratio of the HIMAWARI-8 (Figure 12), whereas such a feature cannot be found for any other communications satellites and broadcasting satellites as shown in Figures 10 and 11, respectively. In fact, the areas of solar panels of the weather satellites are smaller than those of communications and broadcasting satellites as listed in Table 5. It is suggested that the characteristic dip around 4,800 Å is more prominent in the spectrum ratios of HIMAWARI-8 because the amount of light reflected by the solar panels is relatively smaller.

In case of the MTSAT-2 satellite, the number of solar panels are larger than that of the HIMAWARI-8 satellite as also listed in Table 5. Such a difference may make the spectral ratio of the MTSAT-2 rather similar to the communications and broadcasting satellites.

6. CONCLUSION

In order to characterize and classify the artificial satellites based on the optical characteristics, we have observed a number of GEO satellites with the using the GLOWS on the 1.5 m reflector at GAO in Japan.

Our target sample of the GEO satellites consists of two weather satellites, five broadcasting satellites, and four communications satellites as listed in Table 4. These targets are located within the longitude range ±60° from +135° of east longitude, and the orbital inclination smaller than 1°. These spectroscopic observations were performed for several days between 26th April 2016 and 5th June 2016. We first review the results obtained from GLOWS observations as described below:

- All the GEO satellites in our observation sample show the optical spectra resemble to the solar spectrum, which the well-known absorption features such as Hα, Hβ, Na-D, water vapor and oxygen molecule are clearly seen (Figures 6 – 8).
- There is no significant spectral variation in the visible wavelength range during the observation period from April to June (see Figure 8), while atmospheric absorption features varies day by day due to the difference of atmospheric condition of the Earth. The systematic error caused by the atmospheric correction could be negligible (Section 4.2).

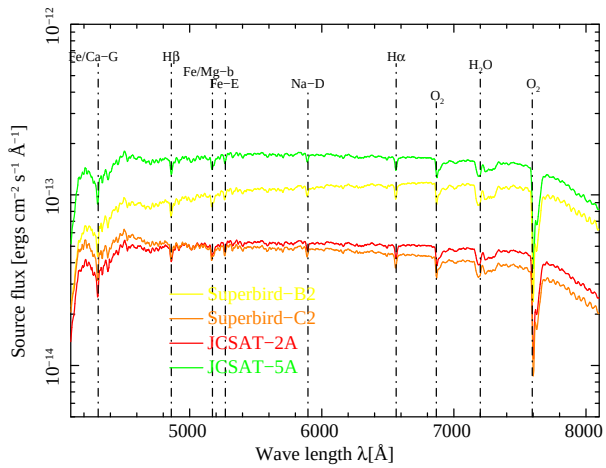

Fig. 6. Energy spectra of communications satellites.

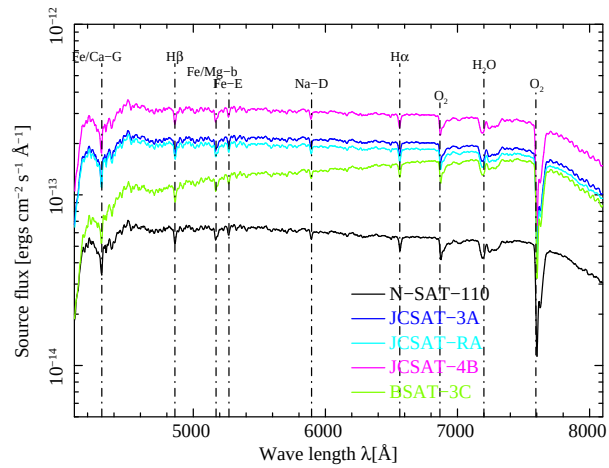

Fig. 7. Energy spectra of broadcasting satellites.

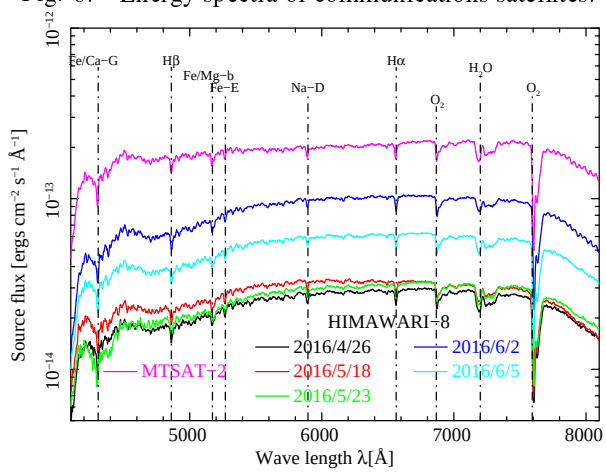

Fig. 8. Energy spectra of weather satellites.

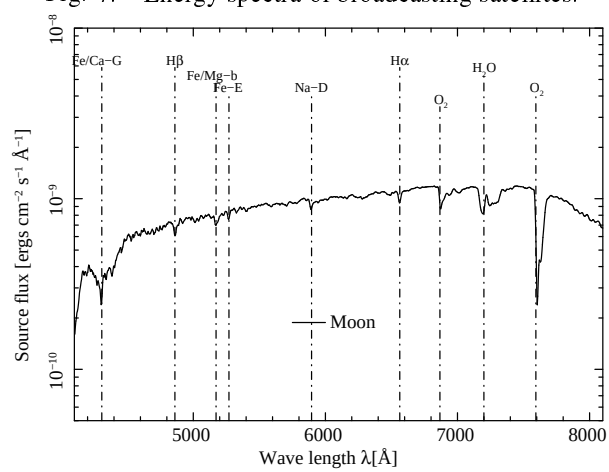

Fig. 9. Energy spectrum of the Moon.

- Spectral features coming from the solar spectrum such as Hα, Hβ and Na-D are canceled in the spectrum ratios calculated by dividing the observed spectra of GEO satellites by a spectrum of Moon which represents the solar spectrum. Any other characteristic features are not found in the spectrum ratios. It indicates that such spectrum ratios are useful enough to investigate the material properties of GEO satellite (Section 5).
- The spectrum ratios show a trend of decreasing as a function of wavelength or a flat distribution for the optical wavelength longer than 4, 500 Å, while they are much affected by atmospheric absorption at shorter wavelengths. It means that the spectral reflectance of satellite materials is bluer than that of the Moon (Section 5).
- A characteristic dip around 4,800 Å is clearly seen only in the spectra of the HIMAWARI-8 (Figure 12). Such a dip feature could not be found in the spectra of communications satellites and broadcasting satellites (Figures 10 and 11), neither even in the spectrum of a weather satellite MTSAT-2 as seen in Figure 13 (Section 5).
- Systematic errors in the analysis of the observed spectra are estimated to be less than 10 % for the wavelength range of $\lambda > 4,500$ Å (Section 4.1).

The reflectivity of solar panels decreases as a function of wavelength as shown in Figure 3. Since the total amount of light reflected by the solar panels is much larger than the light reflected by the bus for most satellites, it is natural that

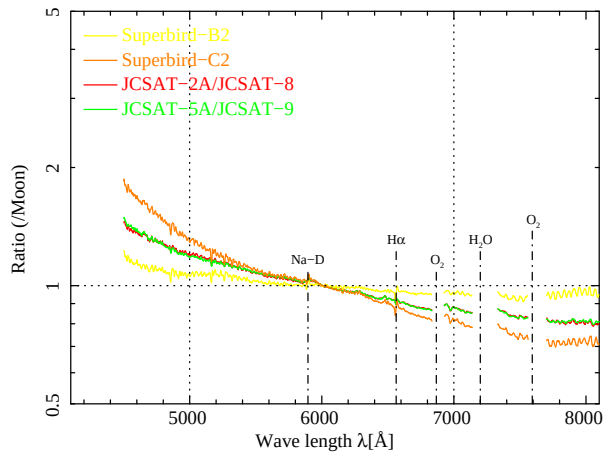

Fig. 10. Spectrum ratios of communications satellites.

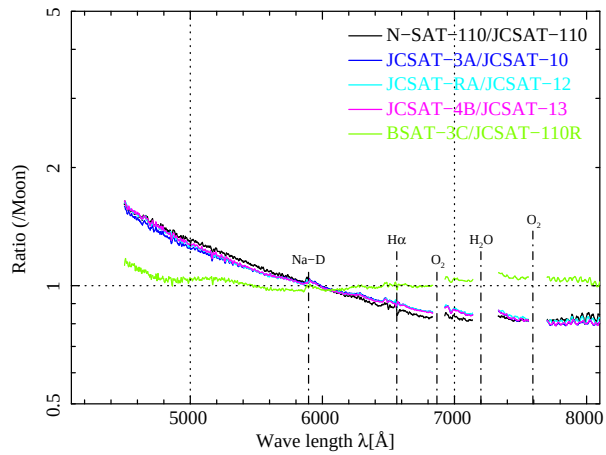

Fig. 11. Spectrum ratios of broadcasting satellites.

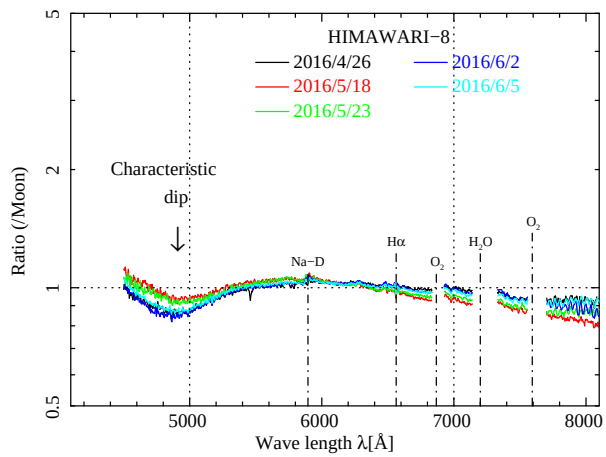

Fig. 12. Spectrum ratios of the HIMAWARI-8 satellite.

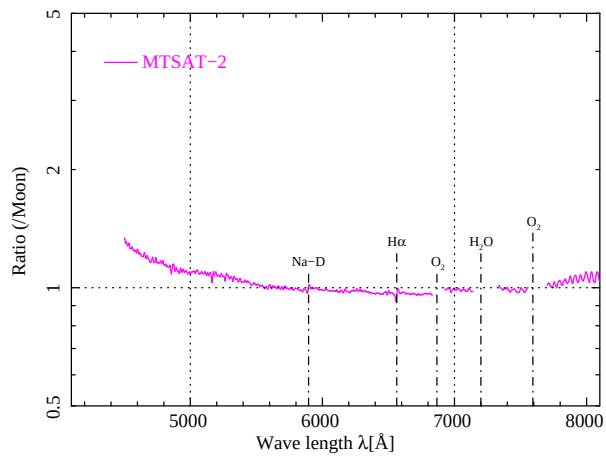

Fig. 13. Spectrum ratio of the MTSAT-2 satellite.

all the observed spectra of the GEO satellites show a decreasing or flat trend against wavelength as seen Figures 10 – 13.

In the case of the HIMAWARI-8, its solar panel area is relatively smaller than those of other satellites due to its smaller energy consumption. It is likely that such a small size of the solar panels of the HIMAWARI-8 causes its unique spectral feature of the dip around 4,800 Å.

As discussed above, we conclude that spectroscopic observation should be a powerful method for identifying and classifying the GEO satellites by their spectroscopic characteristics.

7. REFERENCES

1. Hashimoto, O. et al., Photometric and spectroscopic observations of geostationary satellites with the use of the 1.5 m telescope at Gunma Astronomical Observatory, Spaceguard Research, Vol. 8, 2015.
2. Takahashi, H., Hashimoto, O., Honda, S. and Taguchi, H., 150cm Reflector & Incidental Instruments, ASJ autumn annual meeting. A11c, 2008.

3. New Energy and Industrial Technology Development Organization, Solar radiation spectrum database, http://app0_2.infoc.nedo.go.jp/.
4. Endo, T., Ono, H., Suzuki, J., Ando, T. and Takanezawa, T., Satellite Type Estimation from Ground-based Photometric Observation, 17th AMOS Conference Proceedings, 922–930, 2016.
5. The Society of Japanese Aerospace Companies., Space infrastructure data book: satellite edition, 2011.